Experimental Thermal and Fluid Science 32 (2008) 1620–1627

Contents lists available at ScienceDirect

Experimental Thermal and Fluid Science

journal homepage: www.elsevier.com/locate/etfs

Theoretical, numerical and experimental investigation of centrifugal pumps in reverse operation

Shahram Derakhshan *, Ahmad Nourbakhsh

Department of Mechanical Engineering, Faculty of Engineering, University of Tehran, Tehran, P.O. Box 11365/4563, Iran

ARTICLE INFO

Article history:
Received 1 December 2007
Received in revised form 13 May 2008
Accepted 14 May 2008

Keywords:
Best efficiency point
Characteristic curves
Computational fluid dynamics
Experimental
Pump as turbine

ABSTRACT

When a pump works as a turbine, its hydraulic behavior will be changed. Several methods have been developed to predict the best efficiency of pumps running as turbines but their results are not in good coincidence with experimental data for all pumps. Therefore, study and investigation of hydraulic behavior of pumps in reverse operation can be useful. In this study, the best efficiency point of an industrial centrifugal pump running as turbine was achieved using a theoretical analysis. This method tries to estimate hydraulic components of reverse (turbine) mode using direct (pump) mode. In the next step, the pump was simulated in direct and reverse modes by computational fluid dynamics. 3D full Navier–Stokes equations were solved using FineTurbo V.7 flow solver. Using numerical results, complete characteristic curves of the pump in direct and reverse modes were obtained. For experimental verification of theoretical and numerical results, the pump was tested as a turbine in a test rig. All required parameters were measured to achieve complete characteristic curves of the reverse pump. The theoretical and numerical results were compared with experimental data and some other methods.

1. Introduction

One of the cheap and attractive alternatives in small water-power resources is using pumps in reverse operation. Pumps are relatively simple machines, easy to maintain and readily available in most developing countries. The research on using pumps-as-turbines was started around 1930. With increasing energy demands, it will be more economical to exploit such energy sources in the future. Experiments have shown that in relatively low power outputs, pumps with high technological standards in reverse operation can compete with conventional turbines in respect to maximum efficiency [1]. Pump manufacturers do not normally provide characteristic curves of their pumps working as turbines. This makes it difficult to select an appropriate pump to run as a turbine for a specific operating condition.

Since behavior of a pump running as a turbine changes, prediction of characteristic curves of pump as turbine (PAT) is difficult. Numerous papers have been published on this subject, but there has been comparably limited use of this knowledge. Stepanoff [2], Sharma [3], Wong [4], Gantar [5], Williams [6], Alatorre-Frenk [7], Ramos and Borga [8], Derakhshan and Nourbakhsh. [9], have presented some relations to predicate the best efficiency point (BEP) of a PAT. The results obtained by these relations had almost ±20% deviation from experimental data [10].

Most recent attempts to predict performance of PAT, have been made using computational fluid dynamics (CFD) [11,12]. However, without verifying the CFD results by experimental data, they are not reliable.

In this paper, the best efficiency point of an industrial centrifugal pump running as turbine was achieved using theoretical analysis based on "area ratio" method developed by Williams [5] and Anderson [13]. This method estimates turbine mode hydraulic components based on pump characteristics. Also, this pump was simulated in reverse and direct modes using computational fluid dynamics. 3D full Navier–Stokes equations were solved using FineTurbo V.7 flow solver. Using numerical results, complete characteristic curves of the pump in direct and reverse modes were obtained.

A complete mini hydropower test rig established in laboratory [9] was used for experimental verification of theoretical and numerical results. The simulated centrifugal pump was tested as a turbine in this test rig. All required parameters were measured to achieve complete characteristic curves of the reverse pump. The theoretical and numerical results were compared with experimental data and some other methods.

2. Theoretical analysis

When a centrifugal pump operates as a turbine, flow and rotating directions are reverse. There is one passage with two opposite flows and rotating directions. Using area ratio method [5,13], a

* Corresponding author. Tel.: +98 21 82 08 48 31; fax: +98 21 88 33 86 48.
E-mail address: shhoureh@ut.ac.ir (S. Derakhshan).

0894-1777/$ - see front matter © 2008 Elsevier Inc. All rights reserved.
doi:10.1016/j.expthermflusci.2008.05.004

Nomenclature

a	area, m^2
b	impeller passage width
c	absolute velocity, m/s
D	diameter, m
e	impeller blade thickness, m
g	gravitational acceleration, m/s^2
H	head, m
m	diameter ratio, $\left(\frac{D_2}{D_1}\right)$
N	rotational speed, rpm
n	rotational speed, rps
N_s	specific speed, (m, m^3/s)
P	power, W, kW
Q	discharge, m^3/s
u	peripheral velocity, m/s
w	relative velocity, m/s
z	impeller's blade number

Greek symbols

α	absolute velocity angle (rad)
β	relative velocity angle (rad)
β'	blade angle (rad)
ε	utilization factor
φ	discharge number
μ	slip factor
η	efficiency
π	power number
ρ	density, kg/m^3
ω	rotational speed, rad/s
ψ	head number

Superscript

"	theoretical

Subscripts

b	best efficiency point
e	blade exit
h	hydraulic
i	impeller
l	leakage
m	meridian
me	mechanical
n	net
u	peripheral
p	pump
v	volute
t	turbine

correlation passage between direct and reverse modes of a centrifugal pump may be found. To calculate head, discharge and efficiency of PAT at BEP, hydraulic losses in volute and impeller, mechanical losses related to power losses due to gland packing and bearing cases, disc friction losses in gaps between rotor and stator, volumetric losses related to leakage from clearances between rotor and stator shall be detected.

Fig. 1 shows inlet and outlet velocity triangles in pump and turbine modes. In Fig. 1.a, the gray velocity triangle is related to slip phenomenon (μ is slip factor) on pump mode, since in impeller outlet, real relative flow angle (β_2) is smaller than blade angle (β'_2). The absolute flow angle in position 2, α_2, is approximately the same for both modes of operation in respect to the shape of the volute. A good estimation of this angle is the volute angle, α_v. In reverse mode, the flow angle in blade outlet (β_3) can be assumed close to the blade inlet angle (β'_1) (no whirl at exit). Using momentum theorem and turbine inlet and outlet velocity triangles, Euler head in turbine mode is [2]

$$H''_t = \frac{u_2 c_{u2} - u_3 c_{u3}}{g} \tag{1}$$

Using velocity triangles Eq. (1) can be changed to

$$H''_t = \frac{u_3 Q''_t}{g}\left[\frac{m \cdot \cot\alpha_v}{a_2} + \frac{\cot\beta'_1}{a_1}\right] - \frac{u_3^2}{g} \tag{2}$$

Shockless discharge (Q''_t) is obtained as

$$Q''_t = C_m \cdot a_2 = \frac{u_2 \cdot a_2}{\cot\alpha_v + \cot\beta'_2} \tag{3}$$

To avoid shock losses, the inlet relative velocity angle (β_2) should be as much as possible close to the blade inlet angle.

Flow reaches the impeller after hydraulic losses in volute. These losses must be added to Euler head. Since computing of hydraulic losses is difficult, these losses were estimated using pump mode. The hydraulic efficiency of a pump at BEP can be computed using its overall efficiency [2]:

$$\eta_{hp} \approx \sqrt{\eta_p} \tag{4}$$

Leakage value for pump operation is estimated using Thorne method [14]. Volumetric efficiency is

$$\eta_{lp} = 1 - \frac{Q_{lp}}{Q_p + Q_{lp}} \tag{5}$$

The important parameter is the overall mechanical efficiency including power losses due to disc friction, gland packing and bearing losses. Overall mechanical efficiency is determined using:

$$\eta_{mep} = \frac{\eta_p}{\eta_{lp}\eta_{hp}}.$$

Hydraulic efficiencies in impeller and volute can be defined as

$$\eta_{ip} = \frac{H'}{H''}, \quad \eta_{vp} = \frac{H}{H'} \tag{6}$$

where H'', H', H are Euler, impeller and real heads, respectively. It can be assumed friction losses in impeller and volute are the same, besides, the shock losses in impeller are approximately close to the diffusion losses in volute [5]. So, total losses in volute and impeller are equal: $H'' - H' = H' - H$.

Impeller and volute efficiencies are computed as follows:

$$\frac{H'}{H''} \times \frac{H}{H'} = \frac{H}{H''} \Rightarrow \eta_{hp} = \eta_{ip} \times \eta_{vp}$$

$$\begin{cases} 1 - \eta_{ip} = \frac{H''-H'}{H''} \\ 1 - \eta_{vp} = \frac{H'-H}{H'} \\ H'' - H' = H' - H \end{cases} \Rightarrow (1-\eta_{ip}) = (1-\eta_{vp})\eta_{ip}$$

Then

$$\eta_{vp} = \frac{2\eta_{hp}}{1+\eta_{hp}}, \quad \eta_{ip} = \frac{1+\eta_{hp}}{2} \tag{7}$$

In general, contraction losses are less than expansion losses (in same shapes) [5]. Therefore, volute hydraulic losses in reverse mode are less than direct mode (in same conditions). In other words:

$$1 - \eta_{vt} = k(1 - \eta_{vp}), \quad k < 1 \tag{8}$$

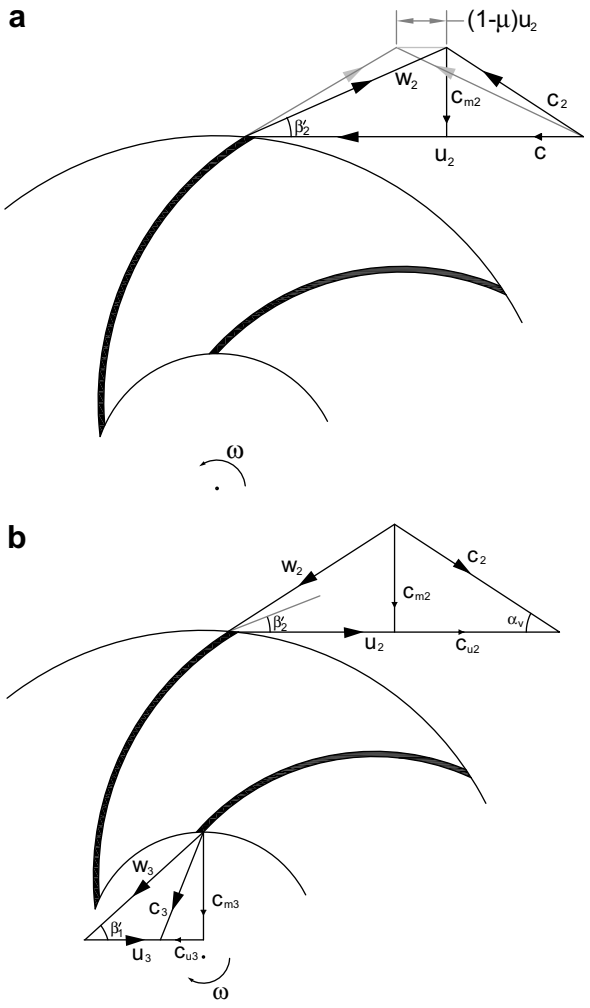

Fig. 1. (a) Pump impeller outlet velocity triangle, (b) turbine impeller inlet and outlet velocity triangles.

There are no empirical equations for the contraction losses and k subsequently. However, Williams [5] assumed: $k = 0.9$.

In turbine impeller outlet, a little no-recovered energy exists in form of kinetic energy. The utilization factor is defined as

$$\varepsilon = \frac{\text{utilized energy by impeller}}{\text{available energy for impeller}},$$

using Fig. 1.a, the utilization factor is:

$$\varepsilon = \frac{H_t''}{H_t'' + \frac{c_{u3}^2}{2g}}, \quad c_{u3} = \frac{Q_t''}{a_1 \tan \beta_1'} - u_3 \tag{9}$$

Real head at BEP of turbine operation is

$$H_t = \varepsilon \cdot \eta_{vt} \cdot H_t'' \tag{10}$$

Turbine discharge at BEP can be evaluated as shockless discharge and leakage value. Using pump leakage value, turbine leakage value can be estimated by

$$Q_{lt} = Q_{lp} \cdot \sqrt{\frac{H_t}{H_p}} \tag{11}$$

Discharge at BEP of turbine mode is $Q_t = Q_t'' + Q_{lt}$.

To calculate maximum efficiency of PAT, total losses shall be evaluated. In same rotational speeds, mechanical losses in turbine and pump modes are the same. Power losses due to leakage are computed as

$$P_{lt} = \gamma \cdot Q_{lt} \cdot (H_t \times \eta_{vt}) \tag{12}$$

Volute power losses of turbine mode are

$$P_{vt} = (1 - \eta_{vt}) \cdot \gamma \cdot Q_t \cdot H_t \tag{13}$$

Using Eqs. (12) and (13), kinetic energy losses in turbine impeller outlet is calculated as

$$P_{et} = (1 - \varepsilon) \cdot (\gamma \cdot Q_t \cdot H_t - P_{vt} - P_{lt}) \tag{14}$$

In same procedure of volute (Eq. (8)), hydraulic efficiencies of impeller in turbine and pump modes are

$$1 - \eta_{it} = 0.9(1 - \eta_{ip}) \tag{15}$$

Hydraulic losses of impeller in turbine mode are evaluated as

$$P_{it} = (1 - \eta_{it}) \cdot (\gamma \cdot Q_t \cdot H_t - P_{vt} - P_{lt} - P_{et}) \tag{16}$$

Turbine net power is

$$P_{nt} = \gamma \cdot Q_t \cdot H_t - P_{vt} - P_{lt} - P_{et} - P_{it} - P_{mt} \tag{17}$$

Turbine maximum efficiency is

$$\eta_t = \frac{P_{nt}}{\gamma \cdot Q_t \cdot H_t} = \frac{\gamma \cdot Q_t \cdot H_t - P_{vt} - P_{lt} - P_{et} - P_{it} - P_{mt}}{\gamma \cdot Q_t \cdot H_t} \tag{18}$$

Using simple assumptions, the BEP of PAT was achieved.

3. Numerical simulation

A 3D model of the pump was generated where the model includes the whole impeller and the volute since a single blade channel model of the impeller alone is not enough to study the circumferential variation of the flow caused by volute (Fig. 2). The model does not include the flow field in the space between impeller hub/shroud and casing nor the sealing gap. The grid size was approximately 700,000 cells. The FineTurbo V.7 flow solver developed by Numeca was used and grid was generated using IGG5.5 for the volute and Autogrid5 for the impeller.

FineTurbo is an integrated software based on finite volume discretization for multi-block structured grids. The multi-block structured grids on the blades were prepared by IGG5.5 and AutoGrid5 [15,16]. The physical model used in the solver is the Reynolds-

Fig. 2. 3D model of simulated centrifugal pump.

Averaged Navier–Stokes equations in rotating frames of reference coupled with various turbulence models and near-wall treatment for low-Reynolds modeling. Without any restriction, the standard high Reynolds k–ε turbulence model can be chosen with extended wall functions [16–18]. The discrete schemes are physically based second order [18]. For fast convergence, mass flow rate, velocity direction, turbulence kinetic energy k and turbulent dissipation ε were imposed at inlet boundary while at outlet boundary condition, static pressure was prescribed. Finally, periodic boundary condition was applied between two blades.

To check if the grid used in the whole pump model is too coarse, simulations were made with one impeller channel and two different grids. The first grid had the same grid coarseness with 70,000 cells for one impeller channel and the second one consisted of about 200,000 cells. The simulation results showed less than 1% difference in calculated efficiencies and heads.

4. Experimental setup

A complete laboratory model of mini hydropower plant was installed in University of Tehran [9] as shown in Fig. 3. The discharge and head for pump working as turbine were generated in the experimental setup by each tested pump. When a pump is working as turbine, a control system is needed to regulate the frequency. The classical governor used for standard turbines are expensive and not always recommended for small hydropower plants. Since these types of plants are more used in remote areas, an electronic load controller with ballast loads was built and used for keeping the frequency of generator in these tests. A conventional synchronous generator was installed to produce electricity. To measure the turbine shaft torque, generator is changed to suspense state and using a scaled arm and several weights, turbine shaft torque can be measured. The discharge was measured by the discharge law and using various orifice plates for each test. Pressures were measured by some barometers ranging from 0 to 5 bar. An industrial low specific speed centrifugal pump with specific speed 23.5 (m, m^3/s) was selected for testing as turbine. This pump has the maximum input turbine shaft power, the maximum head and the maximum discharge of 20 kW, 25 m and 120 l/s, respectively. For the PAT testing, feed pump, several pipes, an orifice, a generator and ballast loads were selected and installed in the test rig. In the PAT applications, it should be considered: that if a generator is coupled directly, a nominal speed corresponding to one of synchronous speeds (e.g. 750, 1000, 1500 or 3000 rpm) should be chosen. For induction generators and also induction motors, slip must be taken into account (the tested pump rotates with

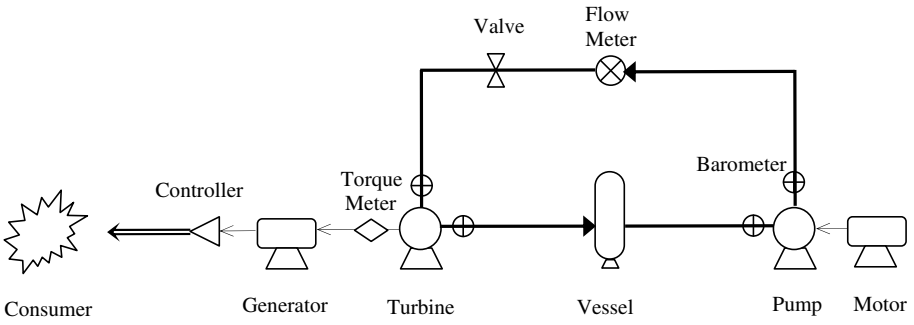

Fig. 3. The mini hydropower established in University of Tehran.

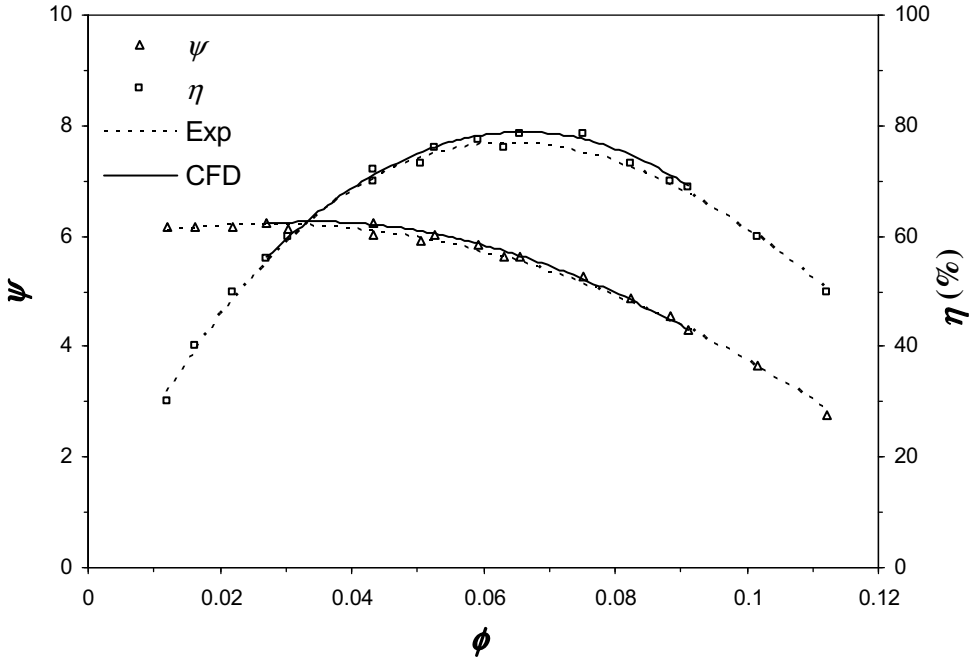

Fig. 4. Measured and numerical head number and efficiency curves of pump mode.

1450 rpm in pump mode). Practically, synchronous generators are usually used. The PAT was tested in N_t = 1500 rpm.

After measuring all parameters, PAT head, discharge, output power and efficiency were obtained. A first-order uncertainty analysis is performed using constant odds combination method, based on a 95% confidence level as described by Moffat [19]. The uncertainty of head, flow rate, power and efficiency are, ±5.5%, ±3.4%, ±5.1% and ±5.5%, respectively.

5. Results

Table 1 shows BEP of the pump predicted by theory and experiment.

Here, ψ, φ, π are defined as

$$\psi = \frac{gH}{n^2D^2}, \quad \phi = \frac{Q}{nD^3}, \quad \pi = \frac{P}{\rho n^3 D^5} \tag{19}$$

Theoretical method predicted 1.1%, 4.7%, 5.25% and 2.1% lower discharge number, head number, power number and efficiency than experimental data at BEP, respectively. The head and power predicted by this method are lower than experimental data due to the volute and the impeller losses evaluation.

The characteristic curves of head, discharge, power and efficiency in pump and turbine modes achieved by experimental and CFD methods were shown in Figs. 4–7. CFD could not simulate leakage, disc friction and mechanical losses since numerical model did not include flow field in the space between impeller hub/shroud and casing nor the sealing gap. To compare CFD results with experimental data, leakage value estimated using Thorne method [14] was reduced from CFD discharges in pump mode. Also mechanical and disc friction losses evaluated using Stepanoff method [2] were added to the pump input power obtained by CFD. The results resemble the experimental data as Figs. 4 and 5. Table 2 shows the BEP of the pump predicted by CFD and experiment. CFD predicted 4.1%, 0.3% and 4.2% and 1.3% higher discharge number, head number, power number and efficiency than experimental data at BEP, respectively.

CFD results for turbine mode were not in good coincidence with experimental data. In turbine mode, the measured discharge is more than real discharge passing from impeller. Using Eq. (11), turbine leakage value was added to CFD discharges of turbine mode. Mechanical and disc friction losses in reverse mode are close to direct mode in same rotational speeds [5]. These losses were reduced from turbine output power computed by CFD. Figs. 6 and 7 show results for PAT.

Table 3 compares the values of BEP_{CFD} and BEP_{Exp} of turbine mode. The deviations of CFD results from experimental data at BEP are −1.1%, −22.9%, −16.4% and +5.5% for discharge number, head number, power number and efficiency, respectively. These deviations maybe in respect to the loss mechanisms in various zones of the PAT control volume and rotational momentum theory across the impeller.

Deviations of the CFD results for the PAT also suggest a lower determination of the net rotational momentum compared to miscalculation of hydraulic losses. However, the miscalculation of losses cannot be ruled out. CFD results of pump mode resemble experimental data. In turbine mode, numerical results and experimental data are not in good coincidence. These deviations are confirmed by other published numerical results [12]. Difference between real geometry and CFD model is only in interaction between volute and impeller according to Fig. 8, since the model does not include flow zone in the space between impeller hub/shroud and casing. There are some miscalculation losses by CFD where head and output power show lower rotational momentum for all regions of discharges. Maybe there are two phenomena in Fig. 8,

Table 1
PAT dimensionless BEP predicted by theoretical method and experiment

	Theoretical	Experimental.	Theoretical error (%)
ϕ	0.089	0.09	−1.1
ψ	9.15	9.6	−4.7
π	0.578	0.61	−5.25
η	0.71	0.725	−2.1

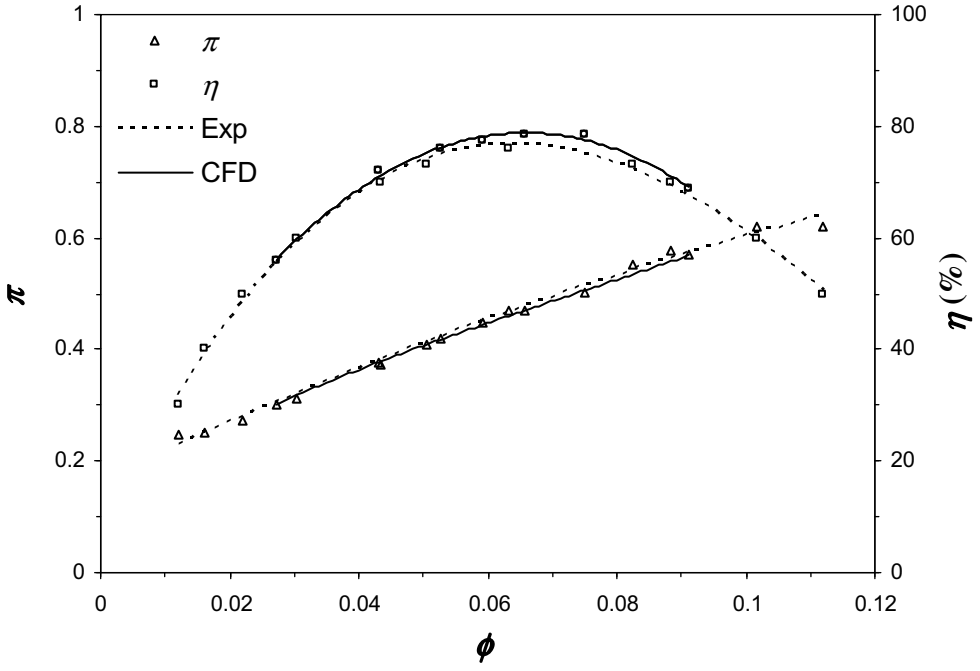

Fig. 5. Measured and numerical power number and efficiency curves of pump mode.

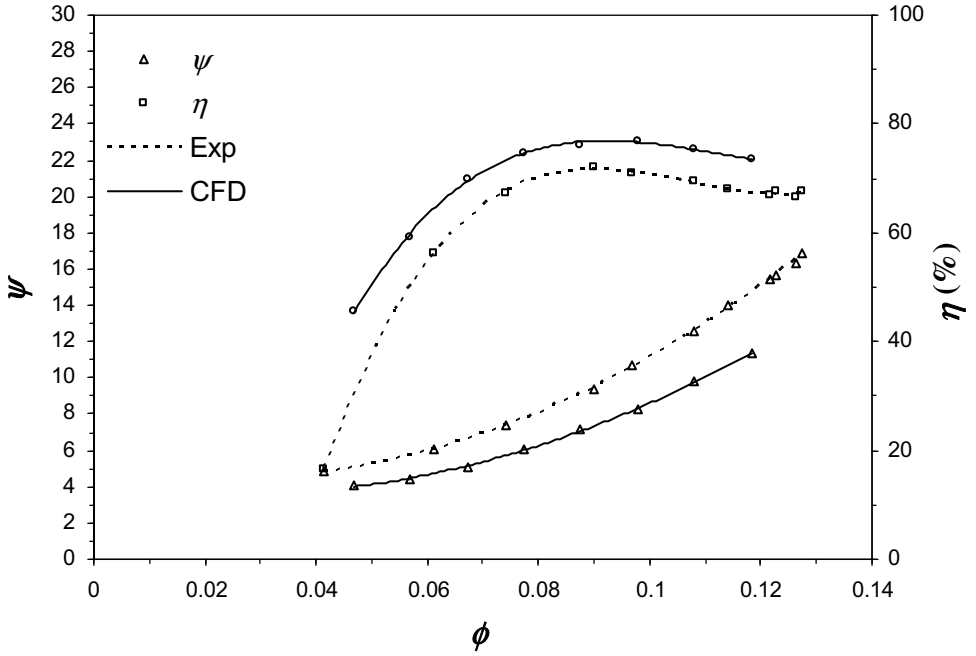

Fig. 6. Measured and numerical head number and efficiency curves of turbine mode.

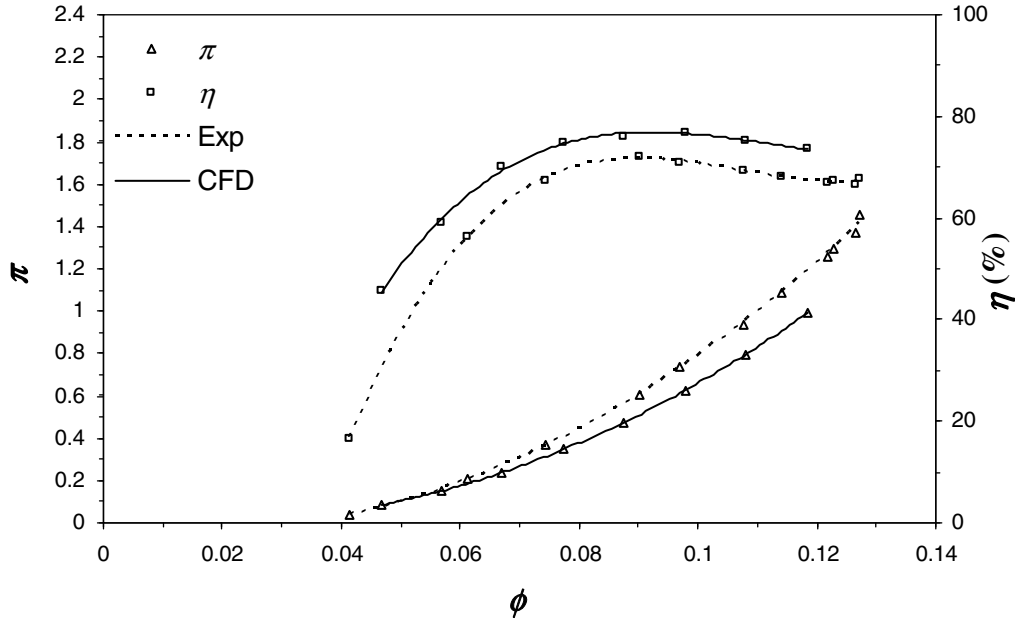

Fig. 7. Measured and numerical power number and efficiency curves of turbine mode.

Table 2
Pump dimensionless BEP predicted by CFD and experiment

	CFD	Experimental	CFD error (%)
ϕ	0.067	0.064	+4.1
ψ	5.66	5.64	+0.3
π	0.49	0.47	+4.2
η	0.78	0.77	+1.3

Table 3
PAT dimensionless BEP predicted by CFD and experiment

	CFD	Experimental	CFD error (%)
ϕ	0.089	0.09	−1.1
ψ	7.4	9.6	−22.9
π	0.51	0.61	−16.4
η	0.765	0.725	+5.5

changing the flow angle in impeller inlet (zone A) and additional losses related to zone B.

In pump mode, flow enters from impeller outlet zone into greater zone as volute inlet. Therefore there are no miscalculated losses

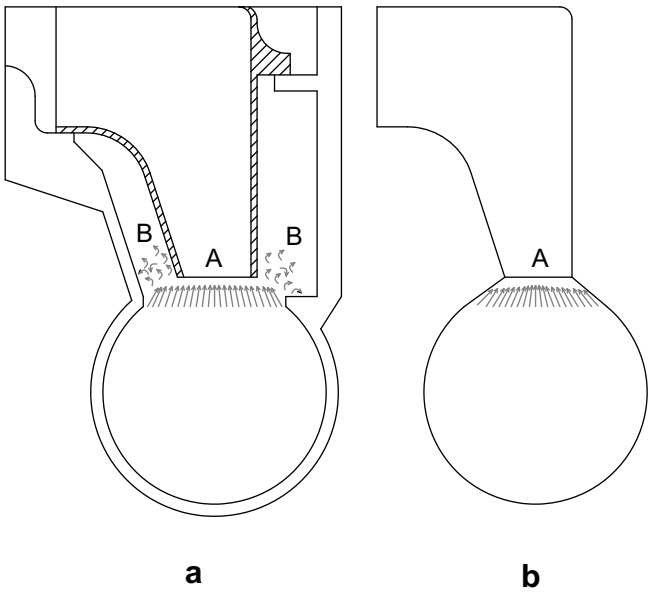

Fig. 8. Volute and impeller interaction: (a) real- and (b) CFD-model.

Table 4
PAT dimensionless part-load point at same discharge predicted by CFD and experiment

	CFD	Experimental	CFD error (%)
ϕ	0.06	0.06	–
ψ	4.6	6.0	−23.3
π	0.18	0.2	−10
η	0.633	0.55	+15.1

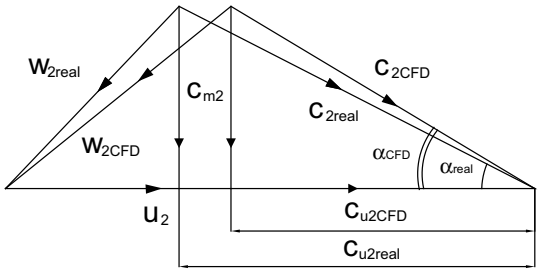

Fig. 9. Turbine mode inlet velocity triangles in real (derived from theory and experimental head and flow) and CFD.

in CFD simulation. On the other hand, the effect of geometric simplification is likely to be greater in turbine mode, because its effect on downstream flow is more than upstream flow, i.e. flow through the impeller. Table 4 shows the deviations of numerical results from experimental data at a part-load point. In simulation, flow enters to the impeller by greater absolute flow angle especially at BEP (Fig. 9). Losses of zone B are miscalculated by CFD in all discharge regions.

Table 5 compares the results of theoretical and numerical methods with experimental data and some other methods. Numerical and theoretical methods estimated the discharge adequately. Predicting the head by theoretical methods is nearly close to experimental data. Numerical method cannot estimate the head accurately. The validity of any prediction method is based on accurate predictions of both head and the discharge accurately.

Stepanoff [2], Sharma [3] and Alatorre-Frenk [7] did not show acceptable results in comparing with the experimental data for both of the head and the discharge.

6. Conclusions

In this paper, a theoretical method was presented to calculate best efficiency point of reverse pump based on pumping mode characteristics (geometric and hydraulic). This method's predicted values are slightly lower than experimental data. In fact, the losses in volute and impeller must be evaluated exactly. In the next step, a centrifugal pump (N_S = 23.5 (m, m^3/s)) was simulated using CFD in direct and reverse modes. To verify numerical results, simulated pump was tested as a turbine in the test rig. CFD results were in good coincidence with experimental data for pump mode not only at best efficiency point but also in part-load and over-load zones. But numerical results were not in acceptable coincidence with experimental data for turbine mode. Turbine head and power values achieved by CFD were lower than experimental data at same discharges. The only difference between direct and reverse modes was in flow and in rotating directions. The difference between real geometry and CFD model was in interaction between volute and impeller since flow zone in the space between impeller hub/shroud and casing was not included in the model. The effect of geometric simplification is likely to be greater in turbine mode, because its effect on downstream flow is more than upstream flow, i.e. flow through the impeller.

Characteristics of best efficiency point predicted by numerical methods were not in good coincidence with experimental data. Future works on CFD application can be improved, since the application of CFD fails in the turbine boundary as proved with this study.

References

[1] J.M. Chapallaz, P. Eichenberger, G. Fischer, Manual on Pumps used as Turbines, Vieweg, Braunschweig, 1992.
[2] A.J. Stepanoff, Centrifugal and Axial Flow Pumps, Design and Applications, John Wiley and Sons, Inc., New York, 1957.
[3] K. Sharma, Small hydroelectric project-use of centrifugal pumps as turbines, Technical , Report, Kirloskan Electric Co., Bangalore, India, 1985..
[4] W. Wong, Application of centrifugal pumps for powers generation, World Pump (1987) , pp. 348–381.
[5] M. Gantar, Propeller pumps running as turbines, in: Conference on Hydraulic Machinery, September 13–15, 1988, Ljubljana, Slovenia, pp. 237–248.
[6] A. Williams, Pumps as turbines used with induction generations of stand-alone micro-hydroelectric power plants, Ph.D.M.E. Thesis, Nottingham Polytechnic, 1992.
[7] C. Alatorre-Frenk, Cost minimization in microhydro systems using pumps-as-turbines, Ph.D.M.E. Thesis, University of Warwick, 1994.
[8] H. Ramos, A. Borga, Pump as turbine: an unconventional solution to energy production, Urban Water 1 (1999) 261–263.
[9] S. Derakhshan, A. Nourbakhsh, Experimental study of characteristic curves of centrifugal pumps working as turbines in different specific speeds, Experimental Thermal and Fluid Science 32 (2008) 800–807.

Table 5
PATs dimensionless BEP predicted by various methods

Pump	Experimental		CFD		Theoretical		Stepanoff [2]		Sharma [3]		Alatorre- Frenk [7]	
N_s (m, m^3/s)	ψ_d/ψ_p	ϕ_d/ϕ_p	ψ_d/ψ_p	ϕ_d/ϕ_p	ψ_d/ψ_p	ϕ_d/ϕ_p	ψ_d/ψ_p	ϕ_d/ϕ_p	ψ_d/ψ_p	ϕ_d/ϕ_p	ψ_d/ψ_p	ϕ_d/ϕ_p
23.5	1.7	1.41	1.31	1.40	1.62	1.39	1.30	1.14	1.37	1.23	1.65	1.63

[10] A. Williams, Pumps as Turbines Users Guide, International Technology Publications, London, 1995.
[11] A. Tomm, A. Braten, B. Stoffel, G. Ludwig, Analysis of a standard pump in reverse operation using CFD, in: 20th IAHR Symposium, 2000, Charlotte North Carolina, USA, Paper No. 5.
[12] A. Rodrigues, P. Singh, A. Williams, F. Nestmann, E. Lai, Hydraulic analysis of a pump as a turbine with CFD and experimental data, in: ImechE, Seminar Proc. of Advances of CFD in Fluid Machinery Design, 2003, London, England.
[13] H.H.Anderson, Anderson, Modern developments in the use of large single entry centrifugal pumps, Proc. Inst. Mech. Eng. 177 (31) (1993).
[14] E.W. Thorne, Design by the area ratio method, in: Sixth Technical Conference of the BPMA, 1979.
[15] AutoGrid v.5 User Guide, Numeca, 2006.
[16] N. Hakimi, Preconditioning methods for time dependent Navier–Stokes equations, PhD thesis, Vrije Universiteit Brussel, 1997.
[17] B. Launder, D. Spalding, The numerical computation of turbulent flow, Computer Methods in Applied Mechanics and Engineering 3 (1974) 269–289.
[18] FineTurbo v.7 User Guide, Numeca, 2006.
[19] R.J. Moffat, Contributions to the theory of single-sample uncertainty analysis, ASME J. Fluids Eng. 104 (1982) 250–260.